15 (2022) 100117

Contents lists available at ScienceDirect

Journal of Non-Crystalline Solids: X

journal homepage: www.sciencedirect.com/journal/journal-of-non-crystalline-solids-x

Space-time rigidity and viscoelasticity of glass forming liquids: The case of chalcogenides

Hugo M. Flores-Ruiz [a], J. Quetzalcóatl Toledo-Marín [b], Cristian Fernando Moukarzel [c], Gerardo G. Naumis [d,*]

[a] Departamento de Ciencias Naturales y Exactas, CUValles, Universidad de Guadalajara, Carr. Guadalajara-Ameca km 45.5, 46600 Ameca, Jalisco, Mexico
[b] Research Institute, BC Children's Hospital, Vancouver, BC, Canada
[c] Departamento de Física Aplicada, CINVESTAV del IPN, 97310 Mérida, Yucatán, Mexico
[d] Departamento de Sistemas Complejos, Instituto de Física, Universidad Nacional Autónoma de México (UNAM), Apartado Postal 20-364, 01000 México, Distrito Federal, Mexico

ARTICLE INFO

Keywords:
Glass transition
Chalcogenides
Viscoelasticity
Relaxation
Rigidity

ABSTRACT

The viscoelasticity of glass-forming fluids contains sustantial information about space-time rigidity. Viscoelasticity and rheology provide alternative experimental, computational and theoretical ways to asses chemical composition effects in the relaxation of supercooled liquids near the glass transition. In particular, the transverse current correlation and transversal dynamical structure factor contain space-time information allowing to relate the dynamical gap of transversal vibrational modes with floppy modes and relaxation times in the liquid. Here, a short revision is made of the subject, including simulations of Tellurium, a typical chalcogenide glass. Our results are similar to those obtained for typical metallic liquids. To rationalize this result, an statistical mechanics analysis in the strain ensemble is performed by using a model that incorporates flexibility and hard-core potentials. This shows that the entropy is akin to a hard-cord fluid as angular bonds only renormalize the entropy if they are not substantially affected by temperature effects. Finally, a comparison is made with Selenium, where bond breaking effects do not allow such a straight-forward treatment.

1. Introduction

The relaxation properties of glass-forming fluids are at the core of the glass transition [1–8], yet many open questions remain [9–17]. A key aspect, important for technological and theoretical reasons, is the minimal cooling speed required in order to make a glass, i.e., the glass-forming ability [2]. Rigidity theory, in which atomic bonds are seen as mechanical constraints, gives excellent insights on how the network topology affects glass-forming ability [3,18,19]. Although it has been used to produce very accurate viscosity models, which allow to relate chemical composition with glass forming ability and viscosity of glass-former melts [20–22], fragility [23,24], the theoretical basis for its success in fluids near the glass transition is in our opinion not yet completely understood. The use of rigidity theory requires the identification of rigid links between nodes, or, in this case, bonds between atoms. Below the glass transition temperature (T_g), this information can be obtained from different experimental sources, or estimated from the chemical composition of the compound. However, at temperatures above the glass transition not all possible links are active, so one needs an operative way to find them. Several aspects of how to answer this question have been addressed using numerical simulations [25], simple models [26–33], or comparisons with empirical laws [34,35]. In the computer simulations of Micoulaut and Bauchy, constraints of rigidity theory are obtained from bond angular excursions [25]. Also, in many cases it is not clear how the dynamical processes at the atomic scale lead to viscous flow and shear relaxation [36,37]. Even below T_g, complications arise, as the local chemical composition is affected by diffusion. Thus, the question of glass heterogenity needs to be addressed in detail as spatial gradients of the chemical composition produce gradients of the average coordination number [32,38].

While for organic glasses there is a vast literature concerning rigidity and rheology [1,39–41], for inorganic glasses, and specially for chalcogenide glasses, frequency-dependent rheology experiments are less numerous [42–46]. Organic glasses present transitions from folded to stretched chains leading to marked viscoelastic effects [41,47]. Viscoelasticity is also present in inorganic glasses, but it is less significant

* Corresponding author.
E-mail address: naumis@fisica.unam.mx (G.G. Naumis).

https://doi.org/10.1016/j.nocx.2022.100117
Received 25 May 2022; Received in revised form 29 August 2022; Accepted 4 September 2022
Available online 6 September 2022

there. G. M. Bartenev adscribed such differences to the much higher C—C bonds rotation flexibility [1].

Recent rheology experiments for inorganic compounds near T_g reveal rigidity at high frequencies and flexibility at low frequencies [43–46]. Rigidity depends on the time-scale under consideration, and the rheological properties of fluids contain valuable information about this dependence. A lack of rigidity is the hallmark of an ideal fluid [48], manifested through the absence of transversal phonons. The associated transverse current fluctuations dissipate through several mechanisms, as for example diffusion. Yet this picture is valid only valid for small fluctuation frequencies (ω) and wavevectors ($\boldsymbol{k}$). Above a certain critical wave vector k_c, relaxation processes are less effective and shear waves appear [49]. Then a viscoelastic response is seen. In fact, it has been experimentally obtained that in the high-frequency (>0.5 THz) range, a liquid can be properly treated within the elastic limit and thus is almost indistinguishable from an amorphous solid [50].

In a previous paper we introduced space-time in rigidity by considering velocity auto-correlation fluctuations, where simulations of glass-forming hard-core systems indicated the relationship between rigidity and viscoelasticity [51]. The dynamical gap in the transversal dynamical structure factor was used as an alternative to test rigidity, in agreement with general ideas that view or understand liquids as perturbed solids [52,53]. For $k < k_c$ fluctuations have almost zero frequency, so these modes can be regarded as floppy. It turns out that k_c can be interpreted as an order parameter in rigidity transitions, which is useful even for the Kosterlitz-Thouless transition [54].

Previous explorations of space-time rigidity were carried out for very idealized systems that do not form strong bonds [51,54]. In fact, for organic glasses it is known that bond angle contributions and polymer chain lengths increase relaxation times [1,39,40]. These factors have not been addressed in space-time dependent constraint theory for inorganic glasses. The aim of this work is to present a short revision of the topic of fluid rigidity, and to apply dynamical rigidity ideas to more realistic glass-forming fluid models.

The layout of this work is the following. In Section 2 we present a general introduction on how to use density-density correlations to test the space-time rigidity of fluids. Therein we present the simulation results for chalcogenides and in particular, for Te. As the results are similar to those obtained for hard-core potential fluids, in Section 3 we present a simple model to rationalize such computational result. Finally, the last section is devoted to the conclusions.

2. Correlations approach to space-time rigidity of fluids

In this section we will discuss how the density-density correlations can provide valuable information about the rigidity of fluids. Then we will turn our attention to compute the response of a typical network glass former. As explained in the introduction, the hallmark of a solid is the presence of rigidity against shear strain and thus the presence of transversal phonons. These collective mode behavior is captured by studying density and velocity correlations, in particular by the transversal part J_T of the atoms current correlation as a function of $\boldsymbol{k}$ and ω, defined as [49,55],

$$J_T(k,\omega) = \int_0^\infty dt e^{-i\omega t} J_T(k,t) \ . \tag{1}$$

where $J_T(k,t)$ is the transversal current density correlation function,

$$J_T(k,t) = \left\langle \left\langle \boldsymbol{j}_T^*(\boldsymbol{k},t) \cdot \boldsymbol{j}_T(\boldsymbol{k},0) \right\rangle_k \right\rangle \ , \tag{2}$$

and the brackets $\langle\langle \ldots \rangle_{\mathbf{k}}\rangle$ represent an ensemble average which is taken after an average over all wave vectors $\boldsymbol{k}$ with the same norm $k = |\boldsymbol{k}|$. The function $\boldsymbol{j}_T(\boldsymbol{k},t)$ is the transversal density current,

$$\boldsymbol{j}_T(\boldsymbol{k},t) = \frac{1}{\sqrt{2N}} \sum_{j=1}^{N} \widehat{\boldsymbol{k}} \times \boldsymbol{v}_j(t) exp\left(i\boldsymbol{k}\cdot\boldsymbol{r}_j(t)\right) \ . \tag{3}$$

where $\widehat{\boldsymbol{k}} = \boldsymbol{k}/k$. In the previous expressions, $\boldsymbol{v}_j(t)$ and $\boldsymbol{r}_j(t)$ are the velocity and position of atom j at time t. The transversal dynamical structure factor ($S_T(k,\omega)$) is related with the transversal current correlation by [49],

$$J_T(k,\omega) = \frac{\omega^2}{k^2} S_T(k,\omega) \tag{4}$$

In a similar way, we define the longitudinal current,

$$\boldsymbol{j}_L(\boldsymbol{k},t) = \frac{1}{\sqrt{2N}} \sum_{j=1}^{N} \left[\widehat{\boldsymbol{k}}\cdot\boldsymbol{v}_j(t)\right] \widehat{\boldsymbol{k}} exp\left(i\boldsymbol{k}\cdot\boldsymbol{r}_j(t)\right) \ , \tag{5}$$

from where $J_L(k,\omega)$ and $S_L(k,\omega)$ are obtained using the correlation $J_L(k,t) = \langle \boldsymbol{j}_L^*(\boldsymbol{k},t) \cdot \boldsymbol{j}_L(\boldsymbol{k},0)\rangle_{\mathbf{k}}$. $J_T(k,t)$ satisfies the transverse part of the linearized Navier-Stokes equation. In its most general expression this is written as [49],

$$J_T(k,\omega) = \frac{2v_0^2 k^2 K_T'(k,\omega)}{\left[\omega + k^2 K_T''(k,\omega)\right]^2 + \left[k^2 K_T'(k,\omega)\right]^2} \tag{6}$$

In the previous expression, $v_0^2 = J_T(k,0)$ while $K_T(k,\omega)$ is a complex memory function, with real $K_T'(k,\omega)$ and imaginary $K_T''(k,\omega)$ parts. The memory function $K_T(k,\omega)$ results from the Fourier transform of the shear viscosity (memory) function $K_T(k,t)$ which satisfies [49],

$$\frac{\partial}{\partial t} J_T(k,t) = -k^2 \int_0^t K_T(k,t-t') \boldsymbol{J}_T(k,t') \tag{7}$$

The simplest model for the shear viscosity function assumes an exponential relaxation of the type,

$$K_T(k,t) = K_T(k,0) e^{-t/\tau_k}, \tag{8}$$

where τ_k is a k-dependent relaxation time. It must satisfy $\tau_0 = \eta/G_\infty(0)$, with $G_\infty(k)$ the k-dependent high-frequency shear modulus and η the viscosity. This expression coincides with the Maxwell relaxation time for a viscoelastic fluid. By taking a Fourier transform of Eq. (8) we obtain

$$K_T'(k,\omega) = K_T(k,0) \frac{\tau_k}{1+\omega^2\tau_k^2} \tag{9}$$

and

$$K_T''(k,\omega) = K_T(k,0) \frac{\omega\tau_k^2}{1+\omega^2\tau_k^2}. \tag{10}$$

Several relaxation processes can be taken into account by using a Prony series made from a superposition of memory functions [56]. To have shear wave propagation and thus rigidity, a resonant condition is required in Eq. (6). Using Eq. (10), we must have $k^2 K_T(k,0) > 1/2\tau_k^2$. As $k \to 0$, $K_T(k,0)$ decreases much faster than τ_k, and eventually the inequality breaks for a critical k_c such that

$$k_c^2 K_T(k,0) = \frac{1}{2\tau^2(k_c)} \ . \tag{11}$$

For $k < k_c$, the maximum of $J_T(k,\omega)$ for a fixed k is at $\omega \approx 0$, while for $k > k_c$ the maximum occurs at $\omega > 0$ and transversal modes appear. This phenomenon is known as the dynamical gap [53]. As an example, in Fig. 1 we present $J_T(k,\omega)$ and $J_L(k,\omega)$ obtained by Y. Zhou and S. Volz from a molecular dynamics simulation of amorphous superionic Li_2S in its liquid state at 1100 K. We refer the reader to the original reference for the simulations details [55]. Fig. 1 a) shows a peak for $J_T(k,\omega)$ that occurs at $\omega \neq 0$. This indicates the presence of transversal modes. In spite of this, there is a substantial nonzero response for $\omega = 0$, indicating that k is close to k_c. On the contrary, Fig. 1 b) shows that for $J_L(k,\omega)$, the

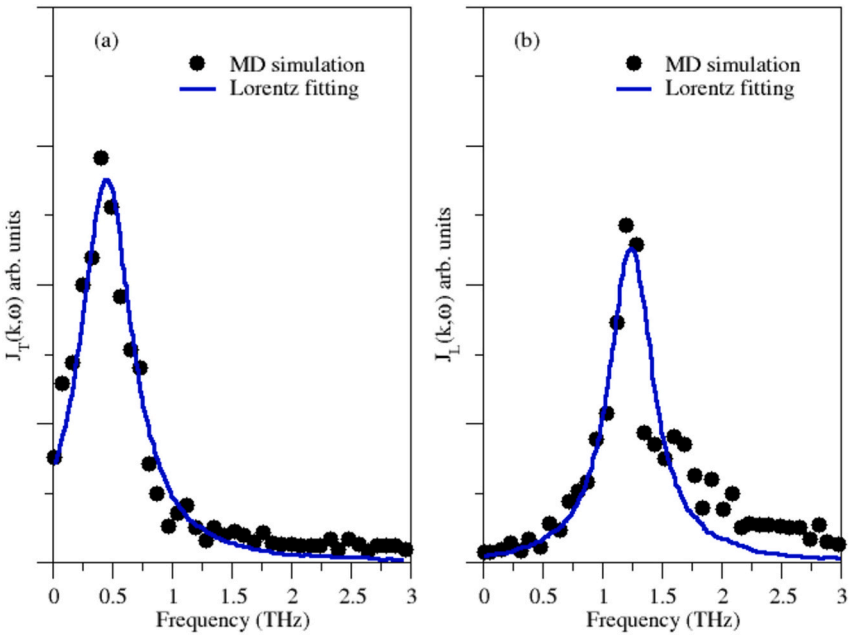

Fig. 1. Panel (a), $J_T(k,\omega)$ for amorphous superionic Li_2S in its liquid state at 1100 K for the lowest wave-vector $\boldsymbol{k} = 2\pi/L$, with L the linear system size. The filled circles were obtained from a molecular dynamics simulation while the solid curves are fittings using a Lorenzian function akin to Eq. (6). These data show a peak near frequency 0.5 THz and a nonzero response for frequency 0 THz. Panel b), $J_L(k,\omega)$. The response is zero for frequency 0 THz. Reprinted with permission from Yanguang Zhou and Sebastian Volz, Phys. Rev. B 103, 224,204 (2021). Copyright 2021 by the American Physical Society.

response at $\omega = 0$ is zero.

Let us now discuss the case of typical network glass formers, in this case chalcogenides. Rigidity effects in such glasses are well known and studied [18,57,58]. Chalcogenides, as for example pure Se or Te, do have floppy modes, that is, $\omega \approx 0$ vibrational modes, which are associated with rotations of dihedral angles in chains [57–60].

For Se, the bonding is of Van der Waals origin, and it is easily destroyed by thermal agitation. For the case of Te, the metallic character is much stronger and has more structure in the liquid [61–63]. This is corroborated in Se viscoelasticity measurements and simulations, which show unequivocally that, in the polymeric fraction, chemical bonds are broken or reformed with an average frequency that depends on temperature [42,63–65]. The dynamic character of bonds poses a problem when dealing with rigidity theory for fluid Se, although in principle this can be solved by using temperature dependent constraints [66]. On the other hand, Te is interesting because it keeps many bonds in the liquid phase and is known to exhibit several anomalous thermodynamic features [67,68]. Due to these reasons, in this work we will study a Te fluid.

Many experiments and simulations reported in the literature study the total dynamical structure factor $S(q,\omega) = S_T(q,\omega) + S_L(q,\omega)$ for chalcogenide glasses [57,69–71]. On the other hand, only a few of those analyze its longitudinal and transversal components separately.

In this work, numerical simulations are used to obtain $J_T(q,\omega)$ and $S_T(q,\omega)$. As Te is quite a complex fluid, instead of assuming a classical force model, we decided to do a quantum-mechanical electronic structure ab-initio molecular dynamics simulation. Therein, forces are computed on-the-fly from quantum-mechanical calculations [72]. A trade-off is thus made between system size and the inclusion of quantum mechanical effects. Here, simulations are made using the Car-Parrinello Molecular Dynamics technique [73] for a system of 300 Te atoms. The NVT ensemble and periodic boundary conditions are employed. The simulation time-step and the fictitious electron mass are 0.024 fs and 1500 a. u., respectively. The valence electrons are considered or included explicitly by means of a Troullier-Martins norm-conserving pseudopotential [74], in a plane wave basis set with an energy cutoff of 20 Ry. The exchange-correlation energy is approached by the PBE functional [75]. The Grimme scheme [76] is then considered to improve the dispersion forces, while the experimental densities [67] are used in order to find or determine the size of the simulation cubic boxes. Table 1 summarizes the temperatures and experimental densities [67] considered. In general, these systems are simulated at temperatures of 2000 K, 1800 K, 1500 K and 1200 K, for a time of 15 ps at each temperature, and subsequently at the target temperatures for a time of 50 ps [77].

Table 1
Temperatures and experimental densities selected for Te in order to determine the size of cubic simulation boxes.

T (K)	ρ_{exp} (gr/cm^3) [67]
773	5.7618
910	5.6708
1173	5.4694

In Fig. 2 we present $J_T(k,\omega)$ for liquid Te at temperature $T = 823$ K using several k values. The lowest k value is $\boldsymbol{k}_1 = 2\pi/L$ where L is the sample length. Fig. 2 shows that for $\boldsymbol{k}_1 = 2\pi/L$, $J_T(k,\omega)$ presents a maxima near $\omega = 0$ for k_1 with a substantial response at $\omega = 0$. For $k_6 = 12\pi/L$ and $k_{10} = 20\pi/L$, the maxima are blue shifted. In spite of this, the system still is flexible as there are floppy modes, seen here in the presence of a response for $\omega = 0$. Similar results are obtained at different temperatures for the liquid phase. These results are similar to those shown in Fig. 1.

To test the validity of the previous results, we can compare our numerical $J_T(k,\omega)$ and $J_L(k,\omega)$ with its experimental counterpart $J(k,\omega)$. In Fig. 3 we present the frequency $\nu = \omega/2\pi$ and energy of the highest peak for $J_T(k,\omega)$, $J_L(k,\omega)$ and $J(k,\omega)$ compared with the results reported from the experiment [78]. Our simulation is in general agreement with such experimental report. Also, the resulting radial distribution functions and speeds of sound show a fair agreement with experiments [71,79].

At this point it is worth while mentioning that the experimental measurement and presence of the transversal rigid response is difficult to asses [80,81]. Convincing experimental evidence is hampered by its loosely resolved and feeble spectral signatures. Moreover, usual spectroscopic methods like Inelastic Neutron (INS) and X-ray Scattering (IXS) are intrinsically unfit to assess the transverse polarization of an acoustic mode in $S(k,\omega)$ unless sided by a parallel computational effort [81]. Thus, although several computer simulations indicate that a shear response should be observed, yet more advanced experimental probes and statistical methods are needed [81]. In the following section we will

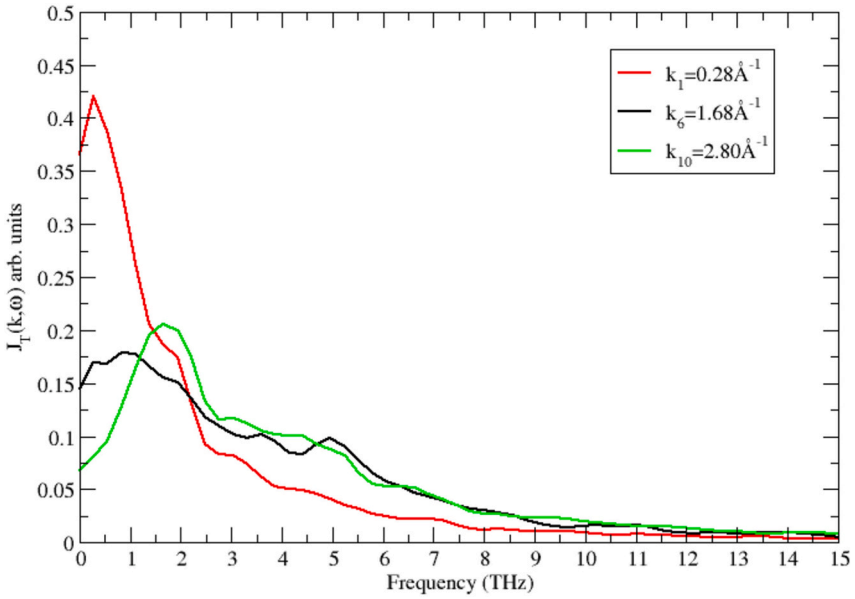

Fig. 2. $J_T(k,\omega)$ for Te at 823 K for the lowest non-zero wave-vector $k_1 = 2\pi/L$, as well as for two other values of k. Notice the reduction in the response for $\omega = 0$ as k grows, indicating fewer flexible modes, identified here with floppy modes. Note that $\omega = 2\pi\nu$, where ν is the frequency.

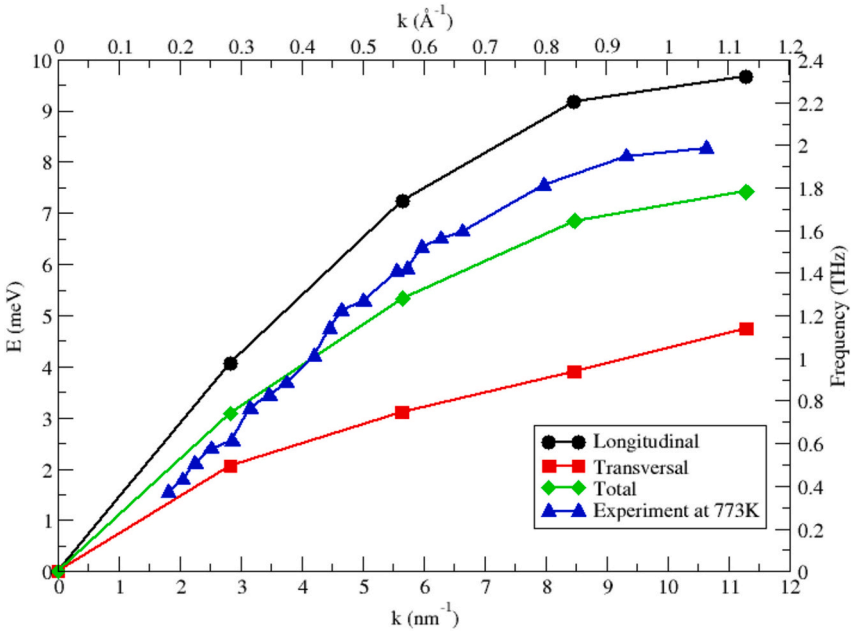

Fig. 3. Frequency (energy) of the maximal current $J_L(k,\omega)$ (black circles) and $J_T(k,\omega)$ (red circles) as a function of ω for Te at 773 K as obtained from the present computer simulation. The maxima of the total current $J(k,\omega)$ (green diamonds) is compared with the experimental results (blue triangles) as reported in Ref. [78]. The order of magnitude and overall behavior is the same, discrepancies are mainly due to the limited size of the system and simulation time. The lines are only a guide to the eye. Note that $\omega = 2\pi\nu$, where ν is the frequency. (For interpretation of the references to colour in this figure legend, the reader is referred to the web version of this article.)

discuss how to interpret the simulation results found in the present section.

3. Statistical mechanics approach to the rigidity of glass former fluids

The surprising lesson from Figs. 1 and 2 is that such results turn out to be quite similar to those obtained for a hard-core potential fluid [51,54]. In fact, earlier works highlighted the striking resemblance of Te viscoelasticity with other metallic liquids like Rb [71,79]. At this point, it is interesting to compare our results with a central experimental work on liquid metals [50]. Giordano and Monaco found that liquid sodium exhibits acoustic excitations of both longitudinal and transverse polarization at frequencies strictly related to those of the corresponding crystal. The only relevant difference between the liquid and the polycrystal was found in the excitations broadening [50]. Our simulation is in agreement with such remarkable experimental finding. Yet, as in liquid Te there is a competition between twofold and threefold local coordination that leads to chain and ring formation [62,68], it is not obvious why it should display a rigidity akin to a hard-core system typical of liquid metals.

In fact, the open question here is why such a network glass former is akin to a hard-sphere fluid. Although we do not attempt to give an exact account of the previous result, we can provide a plausibility argument in the spirit of rigidity theory by adapting arguments from polymer rigidity [82]. We consider first a general Hamiltonian for such a system by including bonding and excluding volume effects,

$$H = H_b + V_{nb}. \tag{12}$$

V_{nb} is an interaction potential that takes into account excluded

volume effects,

$$V_{nb} = \frac{1}{2}\sum_{i,j} u(r_{ij}), \tag{13}$$

where r_{ij} is the distance between atoms i and j and $u(r_{ij})$ is for example, a Lennard-Jones or hard-core potential. H_b is a Hamiltonian that takes into account the kinetic energy and potential due to bonding inside chains and rings (V_b). It can be written by using a flexible model,

$$H_b = \frac{1}{2} g^{\mu\nu} p_\mu p_\nu + V_b, \tag{14}$$

where the Einstein summation rule over repeated indices is implied and the mass is unitary. p_μ, q_μ are suitable momentum and generalized coordinates for each atom, and $g^{\mu\nu}$ is a metric induced by the change of coordinates between the Cartesian and curvilinear sets [83]:

$$g^{\mu\nu} = \delta_{ij} \frac{\partial x^i}{\partial q^\mu} \frac{\partial x^j}{\partial q^\nu}, \tag{15}$$

where $\delta_{i,j}$ is the Kronecker delta-function. Next suppose that there are n degrees of freedom, c constraints and $f = n - c$ flexible coordinates, associated with floppy modes [18]. Constraints can be introduced by assuming harmonic springs with spring constants κ such that $\kappa \to \infty$. The potential energy V_b is written as,

$$V_b = \frac{1}{2}\kappa Y_{A,B} q^A q^B + V_b(q^\alpha), \tag{16}$$

where $A, B = f+1, \ldots, n$ are all labels for the constrained coordinates q^A and q^B, $Y_{A,B}$ a positive-definite matrix that contains the couplings between constrained coordinates, and $\alpha = 1, \ldots, f$ are the labels for the flexible coordinates (q^α). Next we consider a strain-ensemble of chains with prescribed end-to-end vector $\boldsymbol{R}$. The partition function of H_b is given by

$$Z_f(\boldsymbol{R}, T) = (2\pi k_B T)^{(n+c)/2} \kappa^{-c/2} \left|Y_{A,B}\right|^{-1/2} D_f(\boldsymbol{R}). \tag{17}$$

here, k_B is the Boltzmann constant, $|Y_{A,B}|$ the determinant of $Y_{A,B}$ and $D_f(\boldsymbol{R})$ the volume, in configurational space, of the subspace Γ_α defined by all flexible coordinates,

$$D_f(\boldsymbol{R}) = \int_{\Gamma_\alpha} \left|g_{\alpha\beta}\right|_0^{1/2} e^{-V_b(q^\alpha)/k_B T} \prod_{\alpha=1}^{f} dq^\alpha \tag{18}$$

where $|g_{\alpha\beta}|_0$ is the reduced metric associated with the flexible subspace by taking the constrained coordinates at their zero values [83]. For the case of a chain with one free end and fixed bond length a_0, fixed valence bond angles θ_0 and with flexible dihedral angles, we have

$$\left|g_{\alpha\beta}\right|_0^{1/2} = (a_0 sin\theta_0)^{N_M} \tag{19}$$

where N_M is the number of atoms in the chain. In the case of perfectly floppy coordinates, $V(q^\alpha) = 0$, we can recover the result that the free energy and entropy is dominated by a term proportional to the number of floppy modes [84], as from Eq. (17),

$$F \approx -f k_B T ln[\nu(\Gamma_\alpha)], \tag{20}$$

where $\nu(\Gamma_\alpha)$ is an adimensional length,

$$\nu(\Gamma_\alpha) = \int_0^{q^\alpha_{max}} \left|g_{\alpha\beta}\right|_0^{1/2f} dq^\alpha \tag{21}$$

associated with channels in phase-space due to floppy modes [85]. For a polymeric chain, $\nu(\Gamma_\alpha) = (2\pi \sin\theta_0)a_0$ as $f = N_M/3$ (notice that here we are using adimensional units lengths as, for simplicity, the partition function has not been normalized to the Planck constant h). We now calculate the partition function of the whole Hamiltonian Eq. (12) including the non-bonding interactions. The only difference is that now $D_f(\boldsymbol{R})$ is given by

$$D_f(\boldsymbol{R}) = \int_{\Gamma_\alpha} \left|g_{\alpha\beta}\right|_0^{1/2} e^{-[V_b(q^\alpha)+V_{nb}(q^\alpha)]/k_B T} \prod_{\alpha=1}^{f} dq^\alpha. \tag{22}$$

If we consider a hard-core potential, $V_{nb}(q^\alpha) = 0$ whenever hard-spheres do not overlap and $V_{nb}(q^\alpha) = \infty$ otherwise. Then we have

$$Z_f(\boldsymbol{R}, T) = (2\pi k_B T)^{(n+c)/2} \kappa^{-c/2} \left|Y_{A,B}\right|^{-1/2} \left[D_f(\boldsymbol{R}) - D_{f,0}(\boldsymbol{R})\right], \tag{23}$$

where $D_{f,\,0}(\boldsymbol{R})$ is the inaccessible area of Γ_α due to the hard-core interaction.

Now we consider many chains under deformation each identified by an index $l = 1, \ldots, M$ that runs over all chains, each with N_M atoms. In that case, the end-to-end vector $\boldsymbol{R}^0(l)$ of chain l in the initial reference configuration is related to that after the deformation ($\boldsymbol{R}(l)$), by [82].

$$R_i(l) = s_{ij} R^0_j(l), \tag{24}$$

where $R_i(l)$ is the i-th component of $\boldsymbol{R}(l)$ and s_{ij} is the element of a matrix that defines the deformation. If now n and c are the total number of degrees of freedom and constraints considering all M chains, the partition function in the strain ensemble can be written is terms of such deformation as

$$Z_f(s_{ij}, T) = h(T)\left[D_f(s_{ij}) - D_{f0}(s_{ij})\right], \tag{25}$$

where $h(T)$ is a function that only depends on T,

$$h(T) = (2\pi k_B T)^{(n+c)/2} \kappa^{-c/2} \left|Y_{A,B}\right|^{-1/2}. \tag{26}$$

This partition function is made from a purely T-dependent factor times a purely entropic one. In the strain-ensamble, the internal energy is given by [82].

$$U = -\frac{\partial}{\partial\beta} log Z_f(s_{ij}, T) = \frac{dh(T)}{dT}, \tag{27}$$

with $\beta = 1/k_B T$, and the internal stress given by

$$\mathscr{V} T_{ij} = \frac{\partial}{\partial s_{ij}}(U - TS) = -k_B T \frac{d}{ds_{ij}} S. \tag{28}$$

here $\mathscr{V}$ is the volume, T_{ij} is an element of the first Piola-Kirchoff tensor, and S is the entropy, defined as

$$S = -k_B T log\left[D_f(s_{ij}) - D_{f0}(s_{ij})\right]. \tag{29}$$

As we can see, the stress has a purely entropic contribution as long as the chains do not break. This helps to explain why Fig. 2 closely resembles the results of hard-core systems, basically the network effect is to reduce the entropy when compared with the hard-core fluid, and this contribution can be factored out as long as the chains do not reform too much. In other words, the entropy simply gets renormalized. On the other hand, this is not the case if the network has substantial changes with temperature or pressure.

That is the case for systems like Se. For the Se liquid we must consider that: 1) chains, rings, 2) entanglements and 3) orientations are not frozen. The mean length of the Se chain-molecule is about 10^4 atoms near the melting point and decreases quickly with increasing temperature, resulting in about dozens of atoms per chain near the boiling point [64,86,87]. In fact, the dynamic structure factor of Se looks very different from the typical ones for monoatomic liquids [58,63,87]. Recent simulations identified three mechanisms of relaxation and aging near the glass transition [65]. Slowing down of atomic mobility, relaxation driven by diffusion (well described by a defect-enhanced diffusion model) and decay of bonds. These first two effects were identified before on metallic Lennard-Jones glass [88]. In addition, bond breaking without diffusion seems to be a particularity of covalently-bonded

liquids [65]. Chain and ring breaking effects can be captured in a rigidity model by considering that each breaking reduces the constraints [66], as the limit $\kappa \to \infty$ cannot be strictly taken in $Z_f(\boldsymbol{R}, T)$. Concerning entanglements, there are some rigidity models used for organic systems that can be useful to understand inorganic glasses, as e.g. the temporary network model [89]. Yet, their relevance in the context of inorganic glasses needs to be addressed. For example, in liquid Se, the slow relaxation mode is due to entanglement of –Se–Se–Se– chain segments [46]. Chain orientation is another important factor that leads to a plateau in the dynamical properties, falsely adscribed by many authors to entanglement networks [90].

4. Conclusions

In conclusion, we have discussed how viscoelasticity and correlations provide valuable information about rigidity of inorganic network glass forming fluids. This is exemplified here by considering the case of Te. For this system, our Car-Parrinello molecular dynamics simulations indicated that the rigidity is akin to the one seen in hard-core fluids, as for example in typical liquid metals. To rationalize such result, here we used a mechanical model in a strain ensemble. As very strong bonds are kept in the liquid, the entropy of the flexible coordinates renormalizes the whole entropy and thus the fluid behavior is determined by the excluded volume effects of the hard-core potential. Therefore, as long as the network is not substantially reformed in the liquid, the system can be regarded as a hard-core fluid with renormalized parameters.

For other chalcogenides as Se, chain reformation, entanglement and orientation are factors to be included but still it is not clear how to relate them with the experimental and numerical simulation side. The vast literature devoted to the rheology of organic glasses can help enormously [89]. A better understanding of such topics is needed in order to solve the current debate concerning what to expect in the structure of glasses around the rigidity intermediate phase [91,92]. Finally, more research is needed on the dynamical aspects of heterogeneity in rigidity, which is a major hallmark of glassy dynamics [48], and on new probes to experimentally asses the rigidity of fluids [81].

Declaration of Competing Interest

The authors declare that they have no known competing financial interests or personal relationships that could have appeared to influence the work reported in this paper.

Acknowledgments

This work was partially supported by DGAPA-UNAM project IN102620 and CONACyT project 1564464. H. M. Flores-Ruiz gratefully acknowledges the computing time granted by LANCAD and CONACYT on the supercomputer Yoltla/Miztli/Xiuhcoatl at LSVP UAM-Iztapalapa/DGTIC UNAM/CGSTIC CINVESTAV. JQTM acknowledges a Mitacs Postdoctoral Research Fellowship.

References

[1] G.M. Bartenev, The Structure and Mechanical Properties of Inorganic Glasses. By G. M. Bartenev. Translated by [P. Jaray and] F. F. Jaray, Wolters-Noordhoff Groningen, 1970. URL, https://nla.gov.au/nla.cat-vn1842910.
[2] K. Binder, W. Kob, Glassy Materials and Disordered Solids: An Introduction to their Statistical Mechanics, World Scientific, 2011.
[3] A. Varshneya, J. Mauro, Fundamentals of Inorganic Glasses, Elsevier Science, 2019. URL, https://books.google.com.mx/books?id=HBmXDwAAQBAJ.
[4] P.K. Gupta, J.C. Mauro, Composition dependence of glass transition temperature and fragility. i. a topological model incorporating temperature-dependent constraints, J. Chem. Phys. 130 (9) (2009), 094503, https://doi.org/10.1063/1.3077168.
[5] M.L.F. Nascimento, V.M. Fokin, E.D. Zanotto, A.S. Abyzov, Dynamic processes in a silicate liquid from above melting to below the glass transition, J. Chem. Phys. 135 (19) (2011), 194703, https://doi.org/10.1063/1.3656696.
[6] G. Naumis, J. Phillips, Bifurcation of stretched exponential relaxation in microscopically homogeneous glasses, J. Non-Cryst. Solids 358 (5) (2012) 893–897.
[7] P.K. Gupta, D.R. Cassar, E.D. Zanotto, Role of dynamic heterogeneities in crystal nucleation kinetics in an oxide supercooled liquid, J. Chem. Phys. 145 (21) (2016), 211920, https://doi.org/10.1063/1.4964674.
[8] E.D. Zanotto, D.R. Cassar, The race within supercooled liquids—relaxation versus crystallization, J. Chem. Phys. 149 (2) (2018), 024503, https://doi.org/10.1063/1.5034091.
[9] U.R. Pedersen, L. Costigliola, N.P. Bailey, T.B. Schrøder, J.C. Dyre, Thermodynamics of freezing and melting, Nat. Commun. 7 (2016) 12386.
[10] S. Albert, T. Bauer, M. Michl, G. Biroli, J.-P. Bouchaud, A. Loidl, P. Lunkenheimer, R. Tourbot, C. Wiertel-Gasquet, F. Ladieu, Fifth-order susceptibility unveils growth of thermodynamic amorphous order in glass-formers, Science 352 (6291) (2016) 1308–1311.
[11] H.W. Hansen, B. Frick, T. Hecksher, J.C. Dyre, K. Niss, Connection between fragility, mean-squared displacement, and shear modulus in two van der waals bonded glass-forming liquids, Phys. Rev. B 95 (10) (2017), 104202.
[12] T. Gleim, W. Kob, The-relaxation dynamics of a simple liquid, Europ. Phys. J. B-Condens. Matter Compl. Syst. 13 (1) (2000) 83–86.
[13] M. Mezard, G. Parisi, Glasses and replicas, Structural Glasses and Supercooled Liquids: Theory, Experiment, and Applications, 2012, pp. 151–191.
[14] K. Trachenko, V. Brazhkin, Heat capacity at the glass transition, Phys. Rev. B 83 (1) (2011), 014201.
[15] M. Micoulaut, G. Naumis, Glass transition temperature variation, cross-linking and structure in network glasses: a stochastic approach, EPL (Europhys. Lett.) 47 (5) (1999) 568.
[16] J.C. Mauro, D.C. Allan, M. Potuzak, Nonequilibrium viscosity of glass, Phys. Rev. B 80 (9) (2009), 094204.
[17] J.C. Dyre, Colloquium: The glass transition and elastic models of glass-forming liquids, Rev. Mod. Phys. 78 (3) (2006) 953.
[18] J.C. Phillips, Topology of covalent non-crystalline solids i: Short-range order in chalcogenide alloys, J. Non-Cryst. Solids 34 (2) (1979) 153–181.
[19] M. Thorpe, Continuous deformations in random networks, J. Non-Cryst. Solids 57 (3) (1983) 355–370.
[20] J.C. Mauro, Y. Yue, A.J. Ellison, P.K. Gupta, D.C. Allan, Viscosity of glass-forming liquids, Proc. Natl. Acad. Sci. 106 (47) (2009) 19780–19784, https://doi.org/10.1073/pnas.0911705106.
[21] J.C. Mauro, C.S. Philip, D.J. Vaughn, M.S. Pambianchi, Glass science in the united states: current status and future directions, Int. J. Appl. Glas. Sci. 5 (1) (2014) 2–15.
[22] R.L. Siqueira, L.C. Costa, M.A. Schiavon, D.T. de Castro, A.C. dos Reis, O. Peitl, E. D. Zanotto, Bioglass and resulting crystalline materials synthesized via an acetic acid-assisted sol–gel route, J. Sol-Gel Sci. Technol. 83 (1) (2017) 165–173.
[23] D.L. Sidebottom, Fragility of network-forming glasses: a universal dependence on the topological connectivity, Phys. Rev. E 92 (2015), 062804, https://doi.org/10.1103/PhysRevE.92.062804.
[24] S. Sen, J.K. Mason, Topological constraint theory for network glasses and glass-forming liquids: a rigid polytope approach, Front. Mat. 6 (2019), https://doi.org/10.3389/fmats.2019.00213.
[25] M. Bauchy, M. Micoulaut, Atomic scale foundation of temperature-dependent bonding constraints in network glasses and liquids, J. Non-Cryst. Solids 357 (14) (2011) 2530–2537.
[26] A. Huerta, G. Naumis, Relationship between glass transition and rigidity in a binary associative fluid, Phys. Lett. A 299 (5) (2002) 660–665.
[27] A. Huerta, G.G. Naumis, Evidence of a glass transition induced by rigidity self-organization in a network-forming fluid, Phys. Rev. B 66 (18) (2002), 184204.
[28] A. Huerta, G.G. Naumis, Role of rigidity in the fluid-solid transition, Phys. Rev. Lett. 90 (2003), 145701, https://doi.org/10.1103/PhysRevLett.90.145701.
[29] A. Huerta, G.G. Naumis, D.T. Wasan, D. Henderson, A. Trokhymchuk, Attraction-driven disorder in a hard-core colloidal monolayer, J. Chem. Phys. 120 (3) (2004) 1506–1510, https://doi.org/10.1063/1.1632893.
[30] H.M. Flores-Ruiz, G.G. Naumis, Excess of low frequency vibrational modes and glass transition: a molecular dynamics study for soft spheres at constant pressure, J. Chem. Phys. 131 (15) (2009), 154501, https://doi.org/10.1063/1.3246805.
[31] H.M. Flores-Ruiz, G.G. Naumis, Mean-square-displacement distribution in crystals and glasses: an analysis of the intrabasin dynamics, Phys. Rev. E 85 (4) (2012), 041503.
[32] H.M. Flores-Ruiz, G.G. Naumis, J.C. Phillips, Heating through the glass transition: a rigidity approach to the boson peak, Phys. Rev. B 82 (2010), 214201, https://doi.org/10.1103/PhysRevB.82.214201.
[33] H.M. Flores-Ruiz, G.G. Naumis, Boson peak as a consequence of rigidity: a perturbation theory approach, Phys. Rev. B 83 (2011), 184204, https://doi.org/10.1103/PhysRevB.83.184204.
[34] G.G. Naumis, R. Kerner, Stochastic matrix description of glass transition in ternary chalcogenide systems, J. Non-Cryst. Solids 231 (1) (1998) 111–119.
[35] R. Kerner, G.G. Naumis, Stochastic matrix description of the glass transition, J. Phys. Condens. Matter 12 (8) (2000) 1641.
[36] E.L. Gjersing, S. Sen, R.E. Youngman, Mechanistic understanding of the effect of rigidity percolation on structural relaxation in supercooled germanium selenide liquids, Phys. Rev. B 82 (2010), 014203, https://doi.org/10.1103/PhysRevB.82.014203.
[37] W. Zhu, M. Lockhart, B. Aitken, S. Sen, Dynamical rigidity transition in the viscoelastic properties of chalcogenide glass-forming liquids, J. Non-Cryst. Solids 502 (2018) 244–248.

[38] B.S. Almutairi, S. Chakravarty, R. Chbeir, P. Boolchand, M. Micoulaut, Melt dynamics, nature of glass transition and topological phases of equimolar gexasxs100â˜2x ternary glasses, J. Alloys Compd. 868 (2021), 159101, https://doi.org/10.1016/j.jallcom.2021.159101.

[39] R.C. Picu, J.H. Weiner, Stress relaxation in a diatomic liquid, J. Chem. Phys. 108 (12) (1998) 4984–4991, https://doi.org/10.1063/1.475907.

[40] R.C. Picu, G. Loriot, J.H. Weiner, Toward a unified view of stress in small-molecular and in macromolecular liquids, J. Chem. Phys. 110 (9) (1999) 4678–4686, https://doi.org/10.1063/1.478351.

[41] C.W. Macosko, R.G. Larson, Rheology: Principles, Measurements, and Applications, Vch New York, 1994.

[42] G. Faivre, J.L. Gardissat, Viscoelastic properties and molecular structure of amorphous selenium, Macromolecules 19 (7) (1986) 1988–1996, https://doi.org/10.1021/ma00161a035.

[43] Y. Gueguen, V. Keryvin, T. Rouxel, M.L. Fur, H. Orain, B. Bureau, C. Boussard-Plédel, J.-C. Sangleboeuf, A relationship between non-exponential stress relaxation and delayed elasticity in the viscoelastic process in amorphous solids: Illustration on a chalcogenide glass, Mech. Mater. 85 (2015) 47–56, https://doi.org/10.1016/j.mechmat.2015.02.013.

[44] T. Scopigno, S.N. Yannopoulos, F. Scarponi, K.S. Andrikopoulos, D. Fioretto, G. Ruocco, Origin of the λ transition in liquid sulfur, Phys. Rev. Lett. 99 (2007), 025701, https://doi.org/10.1103/PhysRevLett.99.025701.

[45] T. Zhou, Q. Zhou, J. Xie, X. Liu, X. Wang, H. Ruan, Elastic-viscoplasticity modeling of the thermo-mechanical behavior of chalcogenide glass for aspheric lens molding, Int. J. Appl. Glas. Sci. 9 (2) (2018) 252–262, https://doi.org/10.1111/ijag.12290.

[46] W. Zhu, B.G. Aitken, S. Sen, Communication: Observation of ultra-slow relaxation in supercooled selenium and related glass-forming liquids, J. Chem. Phys. 148 (11) (2018), 111101, https://doi.org/10.1063/1.5022787.

[47] H. Takeuchi, R. Roe, Molecular dynamics simulation of local chain motion in bulk amorphous polymers. I. Dynamics above the glass transition, J. Chem. Phys. 94 (11) (1991) 7446–7457, https://doi.org/10.1063/1.460723.

[48] I. Tah, A. Mutneja, S. Karmakar, Understanding slow and heterogeneous dynamics in model supercooled glass-forming liquids, ACS Omega 6 (11) (2021) 7229–7239, https://doi.org/10.1021/acsomega.0c04831.

[49] J.P. Boon, S. Yip, Molecular hydrodynamics, Dover Publications, New York, 1991, pp. 263–265.

[50] V.M. Giordano, G. Monaco, Fingerprints of order and disorder on the high-frequency dynamics of liquids, Proc. Natl. Acad. Sci. 107 (51) (2010) 21985–21989, https://doi.org/10.1073/pnas.1006319107.

[51] J.Q. Toledo-Marín, G.G. Naumis, Viscoelasticity and dynamical gaps: rigidity in crystallization and glass-forming liquids, J. Non-Crystal. Solids: X 3 (2019), 100030, https://doi.org/10.1016/j.nocx.2019.100030.

[52] D. Bolmatov, V.V. Brazhkin, K. Trachenko, The phonon theory of liquid thermodynamics, Sci. Rep. 2 (1) (2012) 421, https://doi.org/10.1038/srep00421.

[53] K. Trachenko, V. Brazhkin, Collective modes and thermodynamics of the liquid state, Rep. Prog. Phys. 79 (1) (2015), 016502.

[54] J.Q. Toledo-Marn, G.G. Naumis, Testing rigidity transitions in glass and crystal forming dense liquids: viscoelasticity and dynamical gaps, Front. Mat. 6 (2019) 164.

[55] Y. Zhou, S. Volz, Thermal transfer in amorphous superionic li_2s, Phys. Rev. B 103 (2021), 224204, https://doi.org/10.1103/PhysRevB.103.224204.

[56] J.C. Mauro, Y.Z. Mauro, On the prony series representation of stretched exponential relaxation, Phys. A: Stat. Mech. Appl. 506 (2018) 75–87, https://doi.org/10.1016/j.physa.2018.04.047.

[57] W. Cooper, S.-T. D. Association, The Physics of Selenium and Tellurium, Elsevier Science & Technology, 1969. URL, https://books.google.com.mx/books?id=jYN-AAAAIAAJ.

[58] W.A. Phillips, U. Buchenau, N. Nücker, A.-J. Dianoux, W. Petry, Dynamics of glassy and liquid selenium, Phys. Rev. Lett. 63 (1989) 2381–2384, https://doi.org/10.1103/PhysRevLett.63.2381.

[59] D. Hohl, R.O. Jones, First-principles molecular-dynamics simulation of liquid and amorphous selenium, Phys. Rev. B 43 (1991) 3856–3870, https://doi.org/10.1103/PhysRevB.43.3856.

[60] M. Foret, B. Hehlen, G. Taillades, E. Courtens, R. Vacher, H. Casalta, B. Dorner, Neutron brillouin and umklapp scattering from glassy selenium, Phys. Rev. Lett. 81 (1998) 2100–2103, https://doi.org/10.1103/PhysRevLett.81.2100.

[61] B. Bureau, C. Boussard-Pledel, P. Lucas, X. Zhang, J. Lucas, Forming glasses from SE and TE, Mol. (Basel, Switzerland) 14 (11) (2009) 4337–4350, 19924068 [pmid], https://doi.org/10.3390/molecules14114337.

[62] J. Akola, R.O. Jones, S. Kohara, T. Usuki, E. Bychkov, Density variations in liquid tellurium: roles of rings, chains, and cavities, Phys. Rev. B 81 (2010), 094202, https://doi.org/10.1103/PhysRevB.81.094202.

[63] J. Kalikka, J. Akola, R.O. Jones, H.R. Schober, Density functional and classical simulations of liquid and glassy selenium, Phys. Rev. B 102 (2020), 104202, https://doi.org/10.1103/PhysRevB.102.104202.

[64] A. Eisenberg, A.V. Tobolsky, Equilibrium polymerization of selenium, J. Polym. Sci. 46 (147) (1960) 19–28, https://doi.org/10.1002/pol.1960.1204614703.

[65] H.R. Schober, Diffusion, relaxation, and aging of liquid and amorphous selenium, Phys. Rev. B 103 (2021), 094202, https://doi.org/10.1103/PhysRevB.103.094202.

[66] C.J. Wilkinson, Q. Zheng, L. Huang, J.C. Mauro, Topological constraint model for the elasticity of glass-forming systems, J. Non-Crystal. Solids: X 2 (2019), 100019, https://doi.org/10.1016/j.nocx.2019.100019.

[67] Y. Kajihara, M. Inui, K. Matsuda, T. Nagao, K. Ohara, Density fluctuations at the continuous liquid-liquid phase transition in chalcogen systems, Phys. Rev. B 86 (2012), 214202, https://doi.org/10.1103/PhysRevB.86.214202.

[68] J. Akola, R.O. Jones, Structure and dynamics in amorphous tellurium and ten clusters: A density functional study, Phys. Rev. B 85 (2012), 134103, https://doi.org/10.1103/PhysRevB.85.134103.

[69] J. Enderby, M. Gay, Liquid te and its alloys, J. Non-Cryst. Solids 35-36 (1980) 1269–1275, https://doi.org/10.1016/0022-3093(80)90372-5.

[70] A. Menelle, R. Bellissent, A.M. Flank, A neutron scattering study of supercooled liquid tellurium, Europhys. Lett. (EPL) 4 (6) (1987) 705–708, https://doi.org/10.1209/0295-5075/4/6/011.

[71] R.V. Gopala Rao, R.J. Venkatesh, Collective excitations and dynamic structure factor of liquid tellurium, Indian J. Chem. 39A (2000) 247–252. URL, http://nopr.niscair.res.in/handle/123456789/25850.

[72] R. Schade, T. Kenter, H. Elgabarty, M. Lass, O. Schütt, A. Lazzaro, H. Pabst, S. Mohr, J. Hutter, T.D. Kühne, C. Plessl, Towards electronic structure-based ab-initio molecular dynamics simulations with hundreds of millions of atoms, Parallel Comput. 111 (2022), 102920, https://doi.org/10.1016/j.parco.2022.102920.

[73] R. Car, M. Parrinello, Unified approach for molecular dynamics and density-functional theory, Phys. Rev. Lett. 55 (1985) 2471–2474, https://doi.org/10.1103/PhysRevLett.55.2471.

[74] N. Troullier, J.L. Martins, Efficient pseudopotentials for plane-wave calculations, Phys. Rev. B 43 (1991) 1993–2006, https://doi.org/10.1103/PhysRevB.43.1993.

[75] J.P. Perdew, M. Ernzerhof, K. Burke, Rationale for mixing exact exchange with density functional approximations, J. Chem. Phys. 105 (22) (1996) 9982–9985, https://doi.org/10.1063/1.472933.

[76] S. Grimme, Semiempirical gga-type density functional constructed with a long-range dispersion correction, J. Comput. Chem. 27 (15) (2006) 1787–1799, https://doi.org/10.1002/jcc.20495.

[77] H. Flores-Ruiz, M. Micoulaut, M.-V. Coulet, A.A. Piarristeguy, M.R. Johnson, G. J. Cuello, A. Pradel, Effect of tellurium concentration on the structural and vibrational properties of phase-change ge-sb-te liquids, Phys. Rev. B 92 (2015), 134205, https://doi.org/10.1103/PhysRevB.92.134205.

[78] M. Inui, Y. Kajihara, S. Hosokawa, K. Matsuda, Y. Tsuchiya, S. Tsutsui, A.Q. Baron, Dynamical sound speed and structural inhomogeneity in liquid te studied by inelastic x-ray scattering, J. Non-Crystal. Solids: X 1 (2019), 100006, https://doi.org/10.1016/j.nocx.2018.100006.

[79] J. Hafner, Dispersion of collective excitations in a metallic glass, J. Phys. C Solid State Phys. 16 (30) (1983) 5773–5792, https://doi.org/10.1088/0022-3719/16/30/008.

[80] A. Cunsolo, A. Suvorov, Y.Q. Cai, The onset of shear modes in the high frequency spectrum of simple disordered systems: current knowledge and perspectives, Philos. Mag. 96 (7–9) (2016) 732–742, https://doi.org/10.1080/14786435.2015.1096975.

[81] A. De Francesco, U. Bafile, A. Cunsolo, L. Scaccia, E. Guarini, Searching for a second excitation in the inelastic neutron scattering spectrum of a liquid metal: a bayesian analysis, Sci. Rep. 11 (1) (2021) 13974, https://doi.org/10.1038/s41598-021-93452-w.

[82] J. Weiner, Statistical Mechanics of Elasticity, Dover Books on Physics, Dover Publications, 2002. URL, https://books.google.com.mx/books?id=2rmPQ4gBDRUC.

[83] M. Fixman, Classical statistical mechanics of constraints: a theorem and application to polymers, Proc. Natl. Acad. Sci. 71 (8) (1974) 3050–3053, https://doi.org/10.1073/pnas.71.8.3050.

[84] G.G. Naumis, Energy landscape and rigidity, Phys. Rev. E 71 (2) (2005), 026114.

[85] G.G. Naumis, Variation of the glass transition temperature with rigidity and chemical composition, Phys. Rev. B 73 (17) (2006), 172202.

[86] R. Keezer, M. Bailey, The structure of liquid selenium from viscosity measurements, Mater. Res. Bull. 2 (2) (1967) 185–192, https://doi.org/10.1016/0025-5408(67)90057-8.

[87] M. Misawa, K. Suzuki, Structure of chain molecule in liquid selenium by time-of-flight pulsed neutron diffraction, Trans. Jpn. Inst. Metals 18 (5) (1977) 427–434, https://doi.org/10.2320/matertrans1960.18.427.

[88] H.R. Schober, Modeling aging rates in a simple glass and its melt, Phys. Rev. B 85 (2012), 024204, https://doi.org/10.1103/PhysRevB.85.024204.

[89] R. Larson, The Structure and Rheology of Complex Fluids, EngineeringPro collection, OUP USA, 1999. URL, https://books.google.com.mx/books?id=Vt9fw_pf1LUC.

[90] D.J. Plazek, I. Echeverria, Don't cry for me charlie brown, or with compliance comes comprehension, J. Rheol. 44 (4) (2000) 831–841, https://doi.org/10.1122/1.551117.

[91] P. Boolchand, X. Feng, W. Bresser, Rigidity transitions in binary ge–se glasses and the intermediate phase, J. Non-Cryst. Solids 293-295 (2001) 348–356, 8th Int. Conf. on Non-Crystalline Materials, https://doi.org/10.1016/S0022-3093(01)00867-5. URL, https://www.sciencedirect.com/science/article/pii/S0022309301008675.

[92] R.F. Rowlands, A. Zeidler, H.E. Fischer, P.S. Salmon, Structure of the intermediate phase glasses gese3 and gese4: The deployment of neutron diffraction with isotope substitution, Front. Mat. 6 (2019), https://doi.org/10.3389/fmats.2019.00133.